



**HAL**  
open science

## Pliocene to Quaternary deformation in the Var Basin (Nice, SE France) and its interpretation in terms of "slow-active" faulting

V. Bauve, Yann Rolland, G. Sanchez, G. Giannerini, D. Schreiber, M. Corsini,  
J.L. Perez, A. Romagny

### ► To cite this version:

V. Bauve, Yann Rolland, G. Sanchez, G. Giannerini, D. Schreiber, et al.. Pliocene to Quaternary deformation in the Var Basin (Nice, SE France) and its interpretation in terms of "slow-active" faulting. Swiss Journal of Geosciences, 2012, 105 (3), pp.361-376. 10.1007/s00015-012-0106-4 . hal-00796152

**HAL Id: hal-00796152**

**<https://hal.science/hal-00796152>**

Submitted on 27 Nov 2021

**HAL** is a multi-disciplinary open access archive for the deposit and dissemination of scientific research documents, whether they are published or not. The documents may come from teaching and research institutions in France or abroad, or from public or private research centers.

L'archive ouverte pluridisciplinaire **HAL**, est destinée au dépôt et à la diffusion de documents scientifiques de niveau recherche, publiés ou non, émanant des établissements d'enseignement et de recherche français ou étrangers, des laboratoires publics ou privés.



Distributed under a Creative Commons Attribution 4.0 International License

# Pliocene to Quaternary deformation in the Var Basin (Nice, SE France) and its interpretation in terms of “slow-active” faulting

Victorien Bauve · Yann Rolland · Guillaume Sanchez · Gérard Giannerini ·  
Dimitri Schreiber · Michel Corsini · Jean-Louis Perez · Adrien Romagny

Received: 30 June 2011 / Accepted: 22 February 2012 / Published online: 18 September 2012  
© Swiss Geological Society 2012

**Abstract** Seismic hazard assessment of active faults in slow orogenic domains is a challenging issue. In this paper we present a multi-disciplinary approach based on a Digital Elevation Model (DEM), 3D-geological modelling, fracture analysis, and strain analysis of pebbles in a Pliocene molasse basin. The basin is cross-cut by “slow-active” faults of the Donaréo and St Blaise-Aspremont fault system. The DEM shows a topographic disturbance emphasized by slope gradients and the drainage system, which is ascribed to the Plio-Quaternary fault trace. Fracturation analysis evidences two fault corridors oriented approximately N150°E and N20°E. Paleo-stress analysis provides orientations similar to those derived from the focal mechanisms of current regional seismicity, with the main stress  $\sigma_1$  oriented N20°E and a  $(\sigma_2 - \sigma_3)/(\sigma_1 - \sigma_3)$  ratio of 0.31. The  $\sigma_2$  versus  $\sigma_3$  permutations are in agreement with ongoing strike-slip deformation at least since the early Pliocene. Discontinuous fracturation and comparison with seismic monitoring on regional active fault zones suggest that shallow seismicity may be expressed by low-magnitude ( $M_w < 4$ ) seismic swarms. Deformation of pebbles occurs

mainly by pressure-dissolution processes. Pebble striation orientations show a bimodal distribution, parallel to the two fault strands. Pebble deformation and the paucity of striated surfaces along the main faults suggests rare seismic deformation and long-lasting aseismic creep processes. Geometrical 3D analysis shows the formation and migration of a Plio-Quaternary basin about 500 metres east of the main fault system, together with folding and tilting of the post-Messinian Pliocene molasse. These observations indicate that the fault remained active from the Pliocene to the Quaternary, and possibly up to the present time. However, the estimates of the minimum slip rate on the faults of about  $0.02 \text{ mm a}^{-1}$  vertical and  $0.03 \text{ mm a}^{-1}$  horizontal are unlikely to produce any significant high-magnitude earthquakes, but rather swarm-like low-magnitude seismicity with long temporal recurrence.

**Keywords** Active faults · Slow tectonics · Fault-basin relationships · Geomorphology · Geological hazards

---

Editorial Handling: A.G. Milnes.

---

**Electronic supplementary material** The online version of this article (doi:10.1007/s00015-012-0106-4) contains supplementary material, which is available to authorized users.

---

V. Bauve (✉) · Y. Rolland · G. Sanchez · G. Giannerini ·  
D. Schreiber · M. Corsini · A. Romagny  
GEOAZUR, UMR 6526, Université de Nice Sophia-Antipolis,  
28 Av. de Valrose, BP 2135, 06108 Nice, France  
e-mail: victorien.bauve@geoazur.unice.fr

J.-L. Perez  
Laboratoire de Nice CETE Méditerranée, 56 Bd. Stalingrad,  
06300 Nice, France

## 1 Introduction

The objective of this paper is to analyze deformations on an exhumed fault system developed in slow tectonic context that might be prolonged up to present times. Such “slow-active” faulting is generally located at the periphery of young orogens and is often thought to be localized along former faults formed in a previously more active tectonic context. Contrary to active faults with high slip rates producing clear seismological features, including a short recurrence period for major seismic events and linear seismic swarms (e.g., Segall and Pollard 1980), such “slow-active” faults produce very low-magnitude seismicity

swarms with a long temporal recurrence of earthquakes (e.g., Crescentini et al., 1999). Conventional seismology does not allow for the monitoring of low-magnitude distal earthquakes of this type and it becomes necessary to put up a dense network of seismometers around the fault (e.g., Courboux et al. 2007; Jenatton et al. 2007). As shown by GPS data (e.g., Delacou et al. 2008) the deformation is slow, and the resulting offset morphologies are reshaped by erosion. The study of such faults by the analysis of Digital Elevation Models (DEM) is complicated because the erosion rate is greater than the displacement rate (Kirby and Whipple 2001; Cushing et al. 2008).

For these reasons, the characterization of active faults in slow-tectonic environments is very challenging. It is important, however, because shallow earthquake events of low magnitude combined with amplifying site effects prove to represent a significant hazard when occurring below densely urbanized areas, as exemplified by the l'Aquila event in April 2009 (Galli et al. 2010).

In this paper, we focus on the active orogenic front of the southwestern Alps (Fig. 1), as it occurs in the suburbs of the city of Nice, where a syn-orogenic basin developed in the Pliocene to Quaternary (Irr 1984), providing evidence for very young (<5 Ma) Alpine deformation (e.g., Sanchez et al. 2010b). There, the presence of active faulting is suspected from subsurface electrical imaging and geomorphology (Bauve et al. 2011; Larroque et al. 2011). However, the duration of deformation and bearing of the fault on seismic hazard are still unconstrained. We propose to combine a morphological DEM study with the analysis of strained pebbles (e.g., Campredon et al. 1977; Hippolyte 2001), striated faults and tecto-sedimentary relationships in order to address the problem of strain localization in the superficial and peripheral part of a very young orogen. An understanding of this fault system which today is located in a densely urbanized area (Nice, Côte d'Azur), has important implications for seismic hazard assessment.

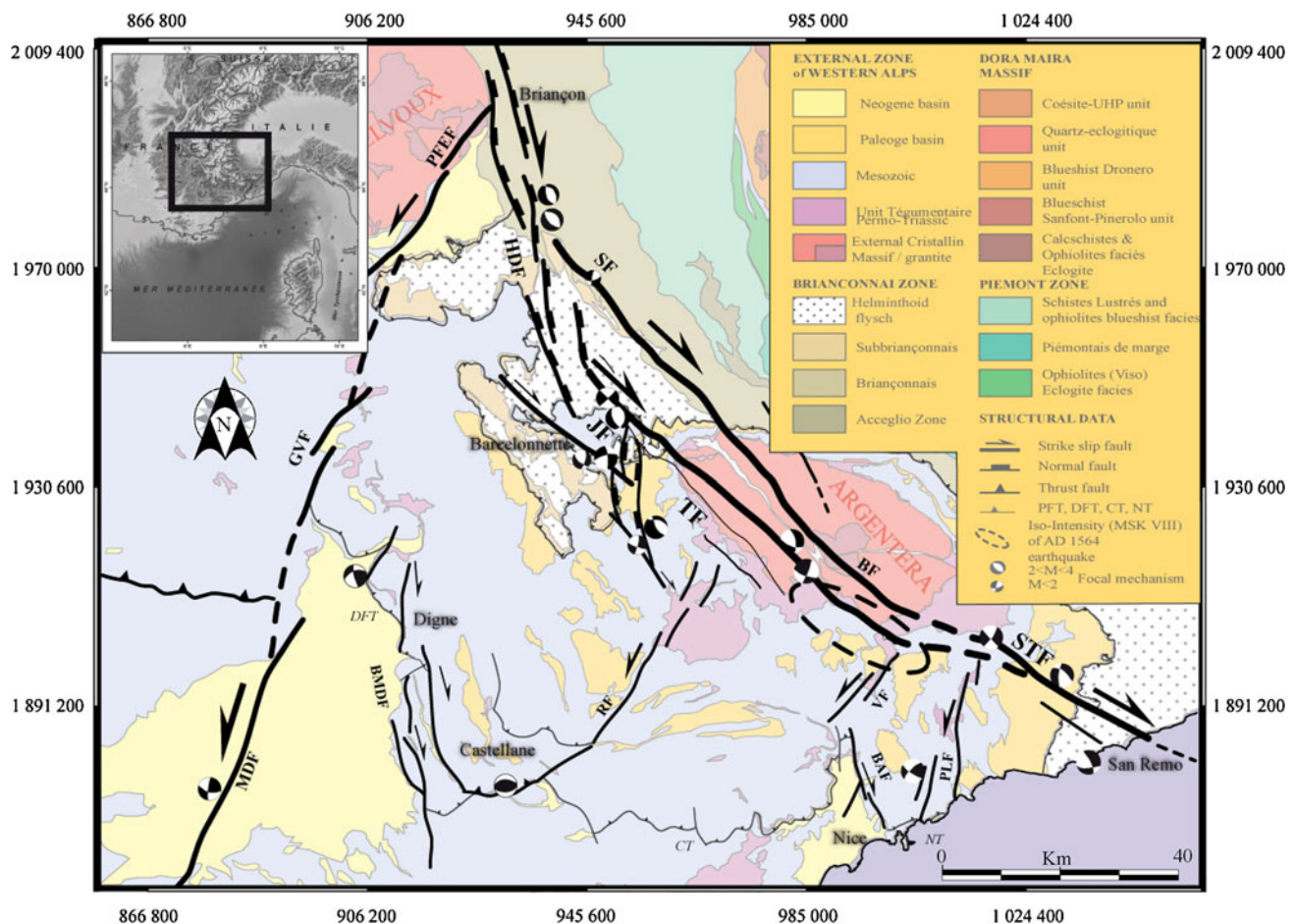


**Fig. 1** Sketch structural map of the Southern Alps, with the main active faults (after Sanchez et al. 2010b, modified). Coordinates are according to the Lambert grid. Fault acronyms are the following: *BAF*

Bercésio and St Blaise-Aspremont fault system (this paper), *JF* Jausiers Fault, *PLF* Peille-Laghet Fault, *STF* Saorge Taggia Fault, *TF* Tinée Fault, *VF* Vésubie Fault

## 2 Geological setting

The study area is located at the southwestern front of the Alps in France (Fig. 1). Recent investigations of active faulting in this region show a relatively continuous N140°E right-lateral fault system bounding the Argentera External Crystalline Massif along the Alpine arc, and minor N20°E left-lateral faults cutting across the Alpine fold and thrust belt (Sanchez et al. 2010b). This active deformation is thought to result from either (1) gravitational collapse of the Alps (e.g., Sue and Tricart 2003) due to rapid change in tectonics mode in the Quaternary (Larroque et al. 2009), (2) climate-induced isostatic rebound and erosion (Cederbom et al. 2004; Champagnac et al. 2007), (3) strike-slip deformation at the boundary of westward extruding Apulia (e.g., Tapponnier 1977), or (4) strike-slip deformation at the boundary of rotating Apulia (e.g., Vialon et al. 1989; Collombet et al. 2002; Baietto et al. 2009; Delacou et al. 2008; Sanchez et al. 2010a, b). Evidence for tectonic activity along this fault system includes ongoing low-magnitude seismicity monitored above the fault in the Jausiers area (Jenatton et al. 2007), and the offset of crystalline glacial morphologies in the Argentera-Mercantour massif (Sanchez et al. 2010a). The widespread evidence for right lateral N140°E strike-slip deformation from ductile conditions at 26–20 Ma (Corsini et al. 2004; Sanchez et al. 2011b) to brittle Mio-Pliocene and Quaternary faulting (Baietto et al. 2009; Sanchez et al. 2010a, b, 2011a) suggests that tectonic motions may be ascribed to the rotation of Apulia since ~26 Ma. However, while major tectonic motions may be accommodated by right-lateral slip along the Argentera-Mercantour Massif by the Jausiers-Tinée faults, probably prolonged by the Saorge-Taggia Fault to the southeast (Fig. 1; Sanchez et al. 2010b), some major and peripheral left-lateral faults show signs of episodic low-magnitude activity, such as that along the Peille-Laghet fault (Courboulex et al. 2007). Unfortunately, this latter fault is hidden by the Paillon valley, and it remains difficult to observe any signs of Plio-Quaternary deformation. However, a similar left-lateral fault system occurs more to the west, along the Donaréo valley in the Pliocene Var Basin and along the boundary of the Nice Arc near St Blaise and Aspremont. There, the fault is observed to crosscut Pliocene to Quaternary sediments (Campredon et al. 1977). The fault is well exposed, and this allows the deformation along such probably ‘secondary order’ strike-slip fault corridors to be analyzed in detail, and to be compared with the main deformation zone running along the side of the Argentera-Mercantour Massif (Sanchez et al. 2010b). Such analysis is of primary importance for evaluating the seismic hazard in such peripheral faults where they crosscut densely urbanized areas. In this paper

we present an analysis of deformation along the western boundary of the Nice Arc, on the south-western Alpine Front. As shown by geological mapping at the scale of the valley (Fig. 2a, b), the Pliocene basin sealed the overall structure of the Nice Arc, implying that most of deformation was already achieved in the Miocene. The Nice Arc is a fold-and-thrust belt formed by the decoupling of the Mesozoic cover from its crystalline basement, related to the exhumation of the Argentera Massif by ~8 Ma (Sanchez et al. 2011a), in front of the Ivrea body indenter (Lardeaux et al. 2006; Schreiber et al. 2010). Later, during the Messinian (~7 Ma), the Var valley was strongly incised due to the rapid lowering of Mediterranean sea level by about 2,000 m (e.g., Clauzon et al. 1996). Infilling of the Pliocene basin was equally rapid, after the restoration of sea level. During Pliocene to Present evolution, the whole margin was uplifted at an approximate rate of 0.3 mm a<sup>-1</sup> (Foeken et al. 2003), which is ascribed to a probable frontal thrust at the base of the continental margin, at the transition to the abyssal plain (Bigot-Cormier et al. 2004).

## 3 Results

### 3.1 Morphological study

The morphological study of the Var Basin was undertaken with a DEM obtained by photogrammetry with a precision of 2 m. The DEM was first treated to eliminate surface artefacts, such as vegetation and buildings, and then it was used to investigate slope patterns in the whole Pliocene Var Basin. The geomorphology of Var valley shows two types of watershed: (1) south of Colomars (Fig. 3, and Online Resource 1), the watershed has a symmetrical shape, with development of a radial system of tributaries, and (2) between Colomars and Aspremont and west of Colomars, the watersheds are asymmetrical and more rectilinear. In the second case, the slopes to the west are steeper and narrower than those to the east of the main stream. The main stream trends N20–30°E, parallel to the main Var valley. We identified a zone of slope anomalies located at the northeast side of the Pliocene basin along the Donaréo valley, where the Donaréo Fault is located (Fig. 3a, c). As shown by DEM analysis, in the whole area underlined in red on Fig. 3, slope gradients are clearly above the average for the Var Pliocene sediments. Slopes steeper than 70° occur in the valley’s central parts, which agrees with increased incision in these areas. It is noticeable that this zone of topographic anomalies occurs also where the flow direction of the Var river turns by about 90° and thus appears to be significantly influenced by the fault

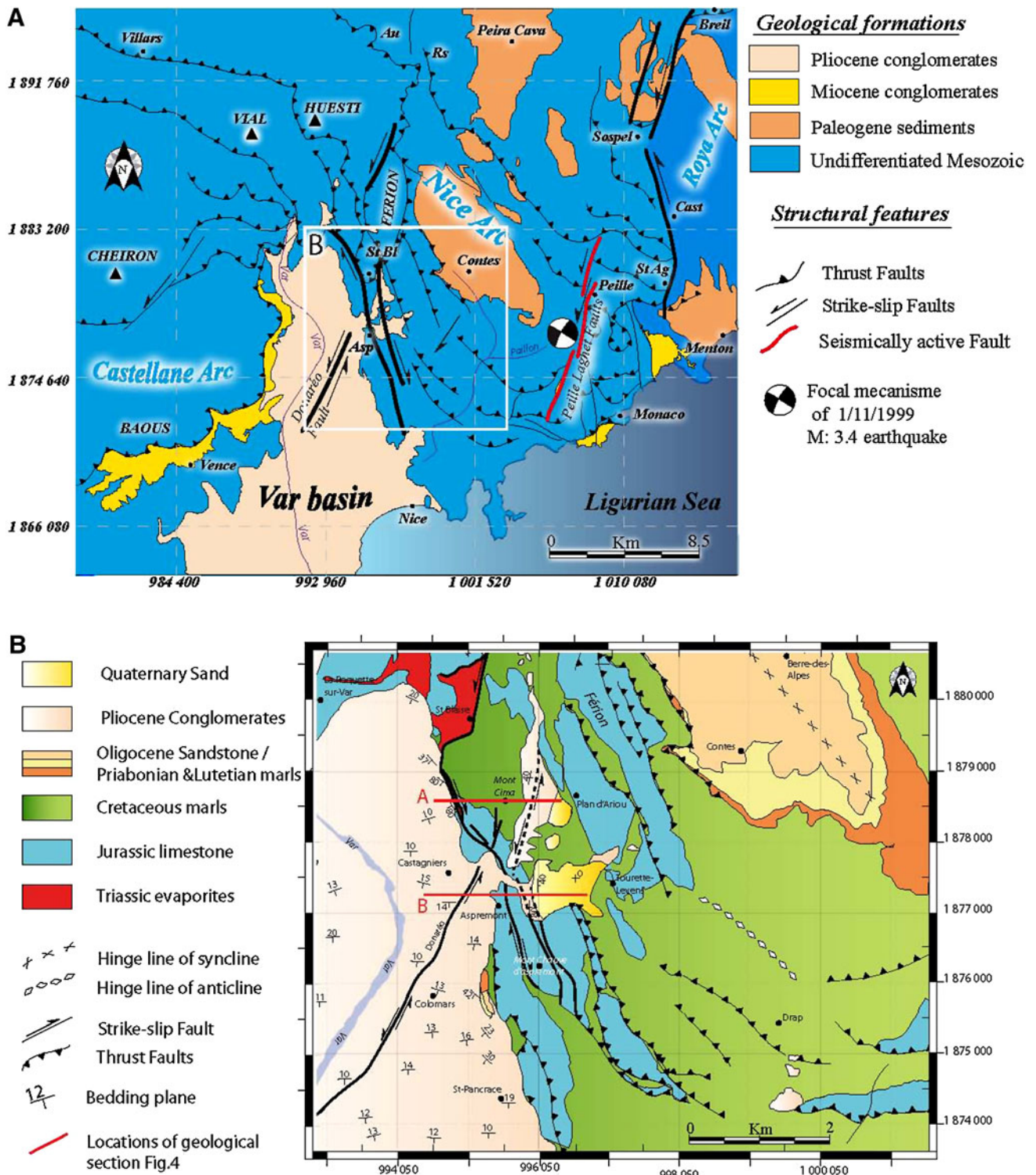


**Fig. 2** a Geological map of the Var Basin and the Nice Arc, with the location of the Peille-Laghet and Donaréo Faults and the main area of detailed study (marked rectangle). b Enlarged structural sketch map

morphology. The secondary water drainage system is also clearly influenced by the fault runoff along the Donaréo and St Sauveur valleys. Secondary valleys merge into the fault instead of being drained into the main Var river.

of the western Nice Arc, showing the relationships between the faults and basins. Note the locations of geological cross-sections of Fig. 4

### 3.2 General structure of the west Nice Arc

The structure of the western Nice Arc is shown on the structural sketch map (Fig. 2b) and illustrated with two

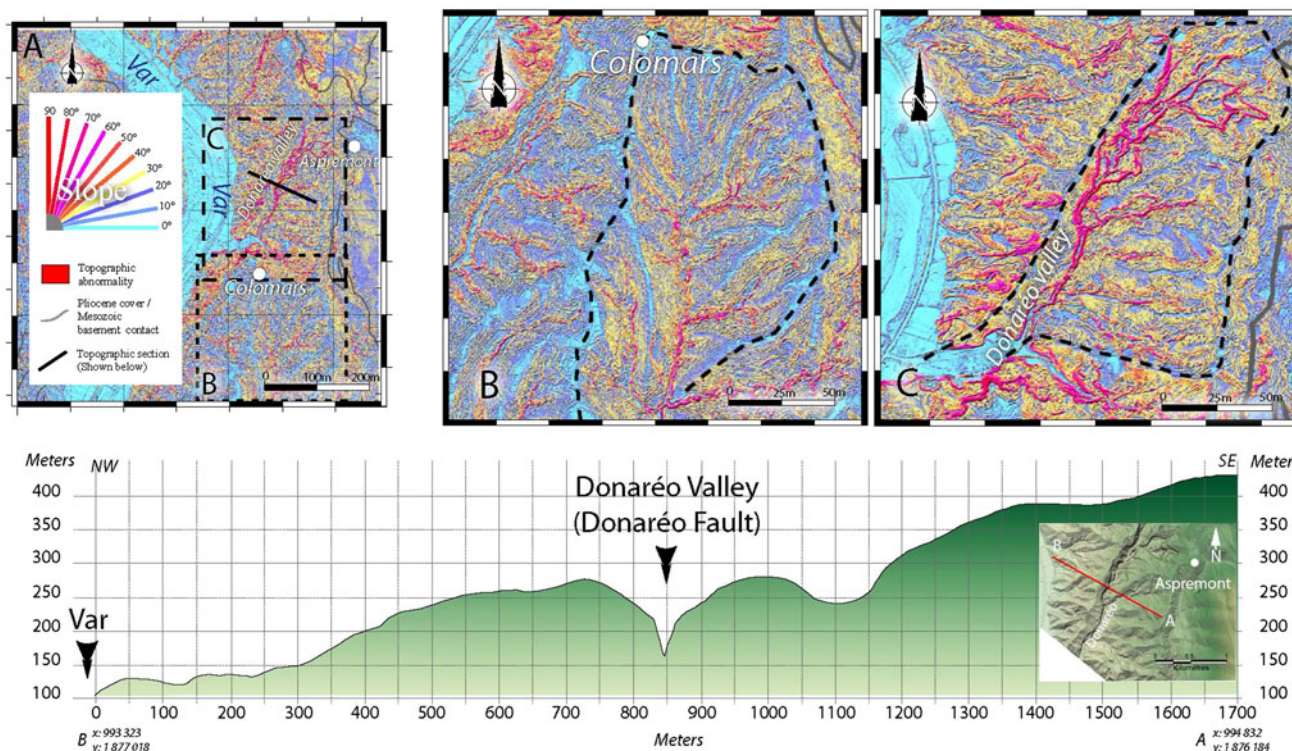


**Fig. 3** Digital Elevation Models (DEMs) of the Var valley and a representative topographic profile across the Donaréo valley. **a** DEM of the Var valley, with slope contour values according to the chart to the left of the figure, below the map. **b** Enlarged DEM of a symmetrical watershed (south of Colomars). **c** Enlarged DEM of an asymmetrical watershed (Donaréo valley). **d** Topographic profile across the Donaréo valley (the location of the section is shown on **a**).

DEMs are shown with *red* shading in the zones of abnormal topography, emphasized by high slope values ( $>40^\circ$ ), mainly along the Donaréo valley. Note the strong influence of the fault runoff in the Donaréo valley on the secondary water drainage system. The topographic signature of the fault is also emphasized by the AB cross-section drawn across the strike of Donaréo valley, below the maps

cross-sections (Fig. 4). These figures show two superposed basins to the east of the western Nice Arc boundary, with: (1) an intramontane Plio-Quaternary basin, characterized by soft lacustrine sandstones (Irr 1984), deposited with an angular unconformity on (2) a Pliocene submarine conglomeratic basin characterized by rounded blocks originating from both the Mesozoic cover and the crystalline basement. To the west of Nice Arc, the folded Mesozoic cover was deeply incised during the Messinian crisis, and was unconformably overlain by a thick pile ( $>1000$  m) of Pliocene molasse of similar composition to that found to the east of Nice Arc (Irr 1984). On this western side, no intramontane Plio-Quaternary basin has been found.

The two (Pliocene and Plio-Quaternary) basins seal most of the fold-and-thrust structure, as shown by their relatively undisturbed bedding, except along the western margin of the Nice Arc (Figs. 2b and 4). The fold-and-thrust belt is mainly ascribed a top-to-S displacement direction along EW-striking thrusts and NS-striking strike-slip faults (e.g., Ivaldi and Guardia 1986; Giannerini et al.

2011). It formed by decoupling of the cover from the crystalline basement along the Triassic décollement.

### 3.3 Bedding plane distribution analysis in the Plio-Quaternary Basin

The Pliocene sediment bedding shows some variability, due to its conglomeratic nature. The general strike of the bedding is  $N86 \pm 13^\circ E$  with a average dip of  $17 \pm 3^\circ S$  (Fig. 5), which is ascribed to an original steep slope during submarine deposition in the Var Canyon (Irr 1984). In general, the Donaréo Fault does not appear to deflect the bedding surface through its path in the core of the Var Basin. However, some deflections appear locally where the Donaréo Fault merges into the Nice Arc (Fig. 2b). Some parallelisation to the Nice Arc boundary is evidenced (Fig. 5) with bedding values significantly out of the  $2\sigma$  envelope of the bedding data. Such deflection of strata is indicative of some strain localisation along the Nice Arc boundary, especially from St Blaise to Aspremont. There, the Pliocene basin is locally overturned with subvertical

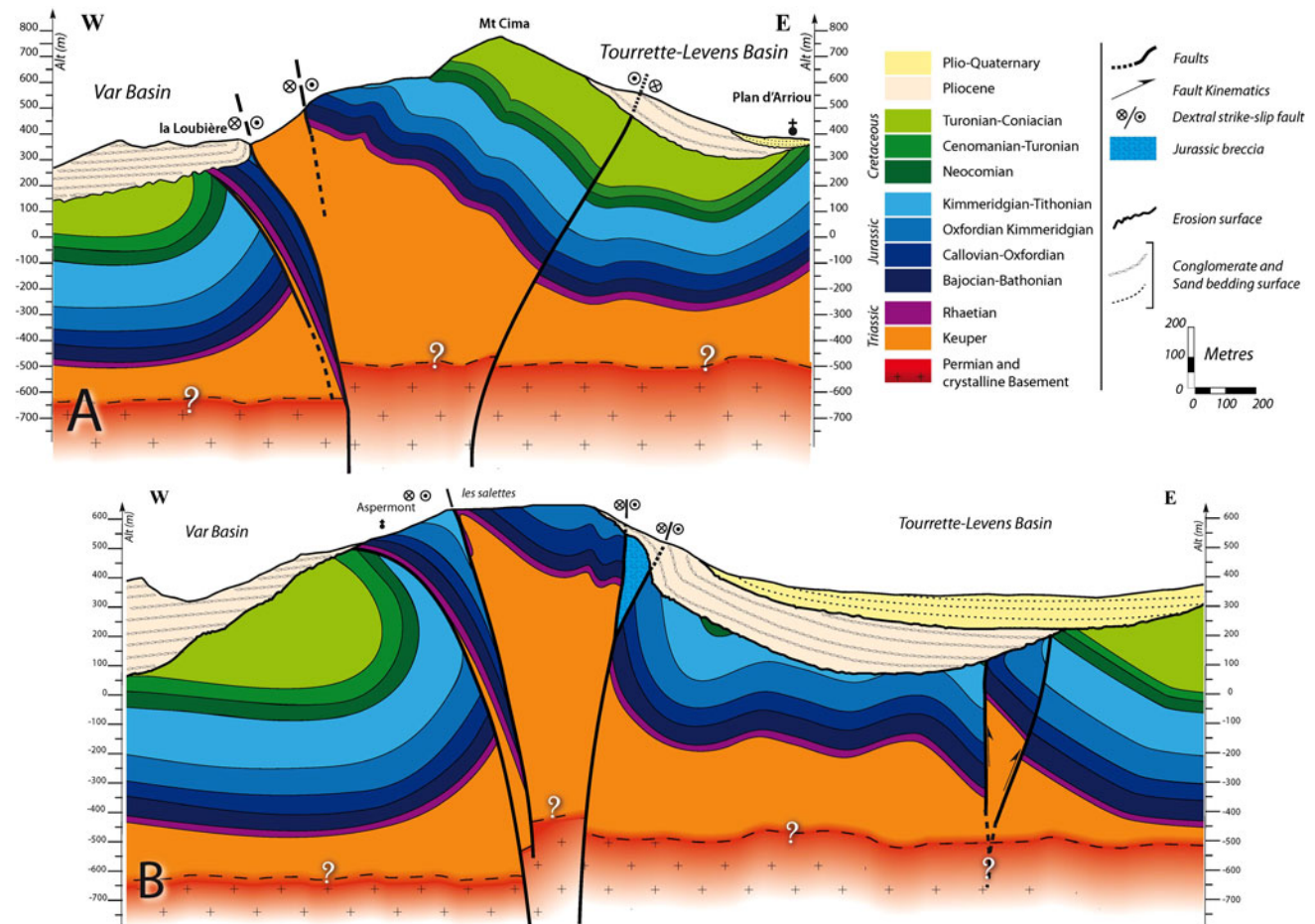


**Fig. 4** Geological cross-sections of the western Nice Arc between Aspermont and St Blaise (location on Fig. 2b). **a** Northern section: La Loubière-Mt Cima-Plan d'Arriou. **b** Southern section Aspermont-Les Salettes. Fold and fault geometries agree with a positive flower-type structure especially in the southern section below 'Les Salettes' (**b**). In both sections, close to 'La Loubière' (section **a**), and east of 'Les Salettes' (**b**), verticalization of the Pliocene emphasizes the Plio-Quaternary activity of the fault system. In addition, note the migration

strata west of 'Mont Cima' (Figs. 4a and 6). Such verticalization also occurs to the east of the Nice Arc, at 'Les Salettes' (Fig. 4b).

In order to better visualize the structure and understand the fault-basin relationship on the east side of the Nice Arc boundary, we have undertaken a 3-D geometrical modelling of this zone (Fig. 14). The basins geometry evidence some differential uplift occurring to the east of Mont Cima (compare Figs. 4a and 5). There, the basal Pliocene conglomerates are tilted by about 80° and overlain by flat lying lacustrine Plio-Quaternary sediments, tilted by 40° along their western boundary. The stratigraphic overturns observed on each side of the Nice Arc boundary in the Pliocene and Plio-Quaternary basins clearly show a post-Pliocene reactivation of a positive flower-type structure (Fig. 4). It cannot be ascribed to initial variability of the

of basin depocenters from the Pliocene to the Quaternary times. Most deformation was acquired before the deposition of Pliocene, as shown by unconformity relationship of the Pliocene basin on the main folded and faulted Mesozoic structure. Cross-cutting of crystalline basement by the strike-slip faults in a 'thick-skinned' tectonic style is mainly suggested by the depth of regional focal mechanisms (c. 5 km) and absence of any significant cover-basement offset since 8 Ma by thermochronology in Sanchez et al. (2011a)

sedimentary strata. This reactivation is also emphasized by the migration of corresponding axial valleys and geomorphologies of about 500 m to the east.

### 3.4 Analysis of faults deformation and kinematics

The Var Pliocene basin was investigated in detail for signs of post-Pliocene deformation. At the scale of this basin, only the zones labelled A, B, C on Fig. 7 show fault surfaces cutting across the Pliocene sediments (cf. Fig. 4). Widespread brittle deformation is observed along the Donaréo valley, which we interpret as the main fault corridor. It is evidenced by numerous metre-scale striated fault surfaces (Figs. 6a and 7) imprinted in the soft Pliocene sediments. No continuous fault has been observed at a scale larger than several meters. It appears that the amount of

fault surfaces decreases rapidly in the surroundings of the main fault corridor, and no fault trace appears at more than about 100 m from the Donaréo valley. In the Donaréo

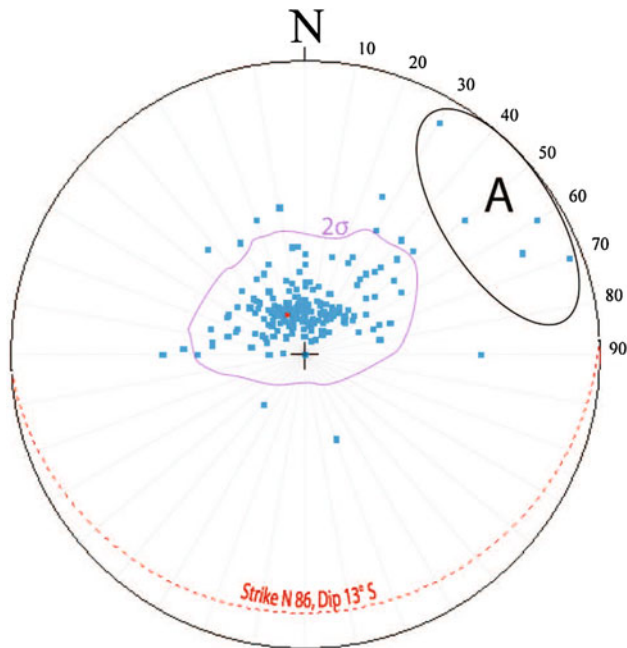


**Fig. 5** Stereogram showing the spread of bedding planes in the whole Var Pliocene Basin (Wulff projection, lower hemisphere). Bedding planes measured close to the Nice Arc boundary lie in the zone marked A. Most data is spread around a mean strike of N86°E and mean dip 13°S. Part of the spread is ascribed to the lithological nature and emplacement of the Pliocene molasses. Molasse emplacement occurred below sea level in a deltaic environment, thus this bedding value corresponds to the untilted original bedding value. A significant spread towards subvertical values is observed (zone labelled ‘A’ in stereogram) in a NW–SE direction. These values were measured along the Nice Arc boundary, west of Mont Cima (Fig. 2b) close to ‘La Loubière’ location (cf. Fig. 4a). Parallelisation of bedding to the western Nice Arc is ascribed to post-Pliocene activity of a dextral + reverse fault (St Blaise-Aspremont Fault)

corridor, the fault surfaces show subhorizontal striation (0–20°) and left-lateral motions, while in the surroundings, some E–W striking faults with reverse motions were identified. Deformation is concentrated along the Mesozoic basement-Pliocene cover to the north to the west of Mont Cima (St Blaise-Aspremont Fault; A in Fig. 7), while evidences of faults affecting the Pliocene are also seen to the east of Aspremont and Mont Cima. These fault occurrences are interpreted as discontinuous fracturation occurring along the main fault corridors, mainly striking N20–30°E and N150–160°E, respectively. Inversion of fault-striation data by the method of Angelier (1990) was only possible for the Donaréo Fault corridor due to a lack of sufficient fault density in the other areas. It provided a stress tensor featured by N22°E compression and subvertical extension axes (Fig. 8). The ratio  $\sigma_2 - \sigma_3 / \sigma_1 - \sigma_3$  is 0.31, which suggests that  $\sigma_1$  is significantly greater than  $\sigma_2$  and  $\sigma_3$ . In such cases, permutations between  $\sigma_2$  and  $\sigma_3$  are likely (Hu and Angelier 2004), as are frequent in strike-slip contexts, and already described along the Jausiers-Tinée Fault (Sanchez et al. 2010b). This result suggests that all the faults (reverse and strike-slip) are generated by a similar  $\sigma_1$ , and permutations of  $\sigma_2 - \sigma_3$ , in an overall similar strike-slip context. Similar results are obtained with the ‘Diedres Droit’ method (Arthaud 1969), computed for all the faults collected around and within the Donaréo Fault (Fig. 8b). On average, this method gives a direction for compression of N03 ± 7°E, while extension axes are spread in a plane perpendicular to compression. Accordingly, computations done with the ‘Diedres Droit’ method in the other fault segments also show N–S compression, ranging from N170°E and N20°E, and extension direction varying along the plane perpendicular to compression (Fig. 8). These data are thus also in agreement with permutations of  $\sigma_2$  and  $\sigma_3$ . Such stress directions and

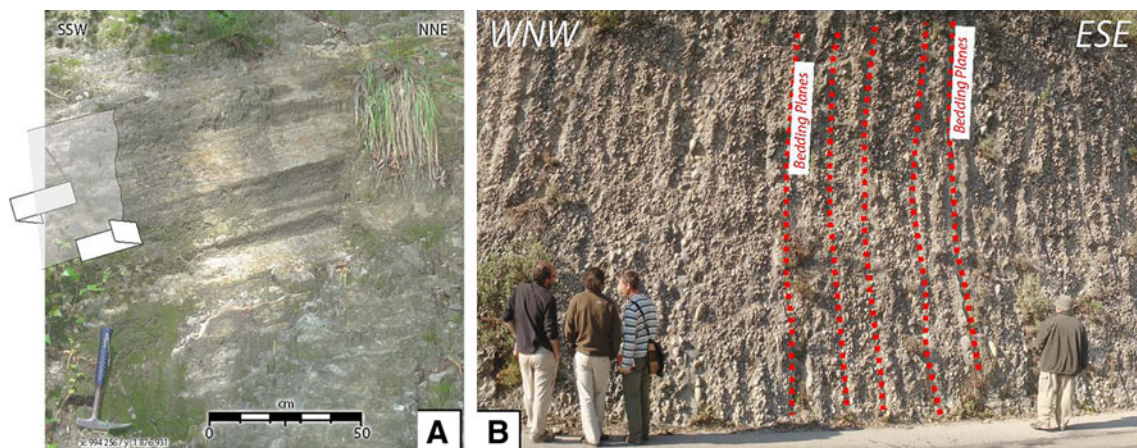


**Fig. 6** Field photographs of faulted and tilted Var Basin Pliocene molasse-type sediments. **a** Photo representative of the most common fault deformation feature in studied area, showing a striated fault

plane with sinistral sense of motion in Donaréo valley. **b** Verticalized Pliocene strata along the St Blaise-Aspremont Fault (at ‘La Loubière’, west of Mont Cima, Fig. 4a)

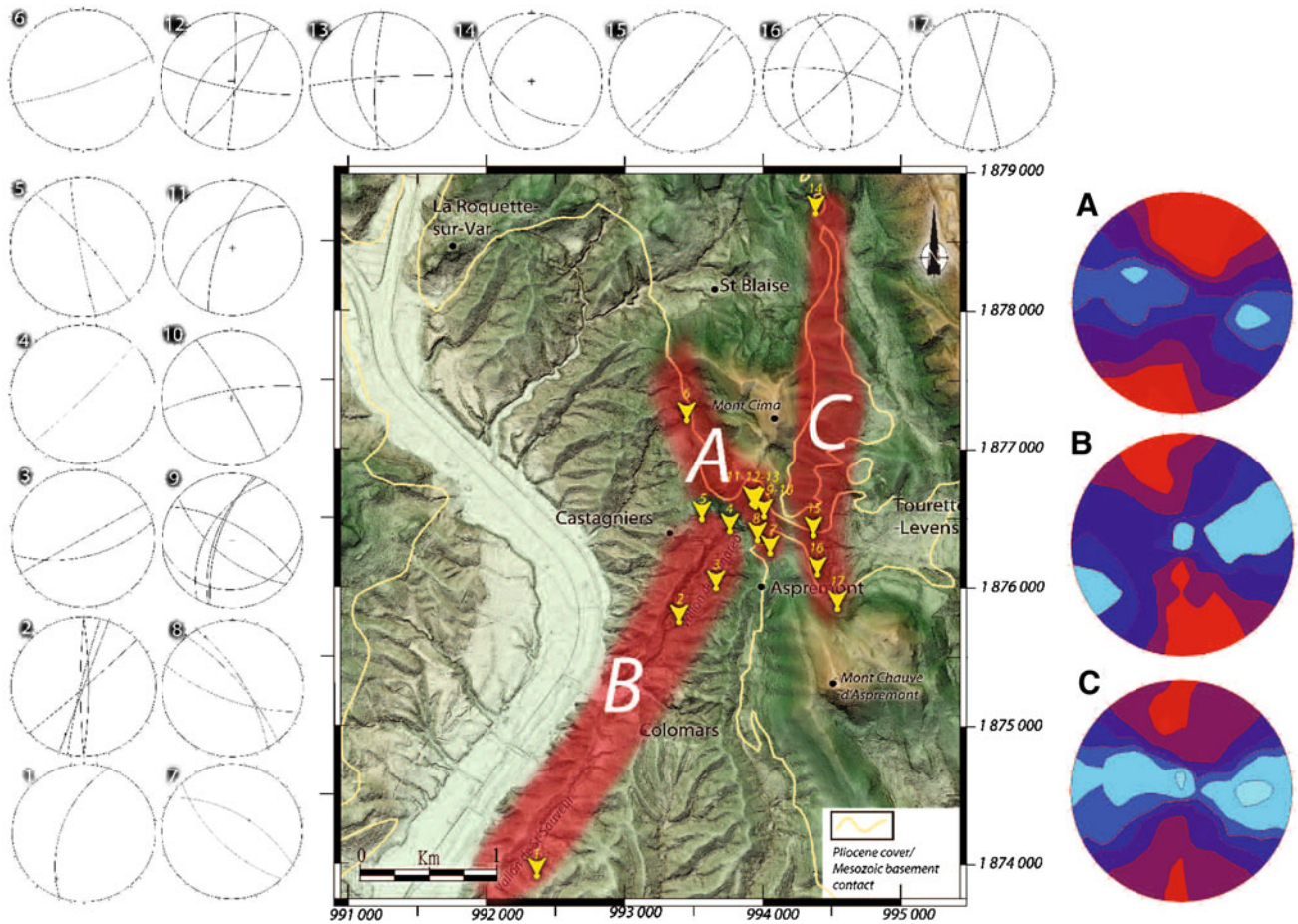


**Fig. 7** Locations of measured faults and corresponding stereonets (1–17). A, B and C are computations of main deformation axes by the ‘Diedres Droits’ method of Arthaud (1969) using all the measured faults in each of the A–B–C zones on the map (red compressional and blue extensional)

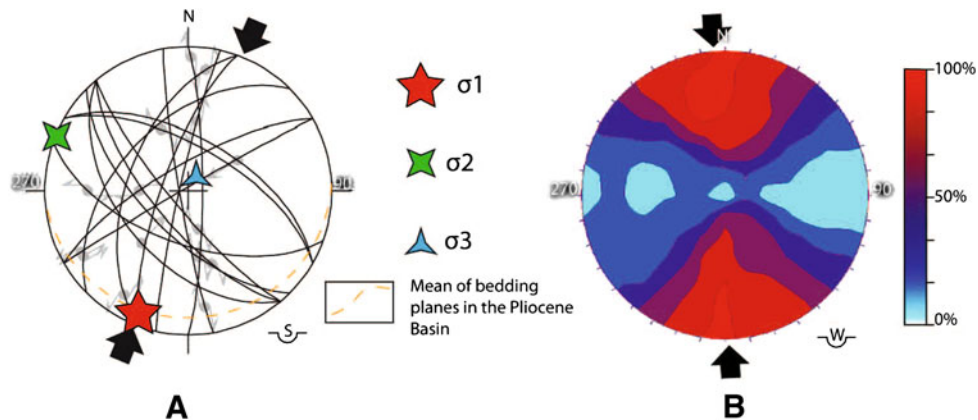


**Fig. 8** Stereograms showing **a** results of inversion of fault-striation data measured in the Donaréo Fault using the Angelier (1990) method, **b** results of ‘Diedres droits’ inversion computed from all the fault-striation data shown in Fig. 8. Results provided by punctual stress inversion of Angelier and results at the scale of the study area

permutations are observed at a regional scale (e.g., Sanchez et al., 2010b) and suggest a coherent tectonic context from the north-western boundary of the Argentera-Mercantour Massif to the Mediterranean coastline.

by ‘Diedres droits’ inversion are similar, characterized by N–S compression. Spread of T axis probability on the E–W direction of ‘Diedres droits’ inversion results suggests possible permutations between  $\sigma_2$  and  $\sigma_3$ , as also indicated by the stress inversion results (see text for details)

### 3.5 Pebble deformation analysis

Investigations conducted across the Donaréo Fault, the Nice Arc boundary and Tourette-Levens Basin show

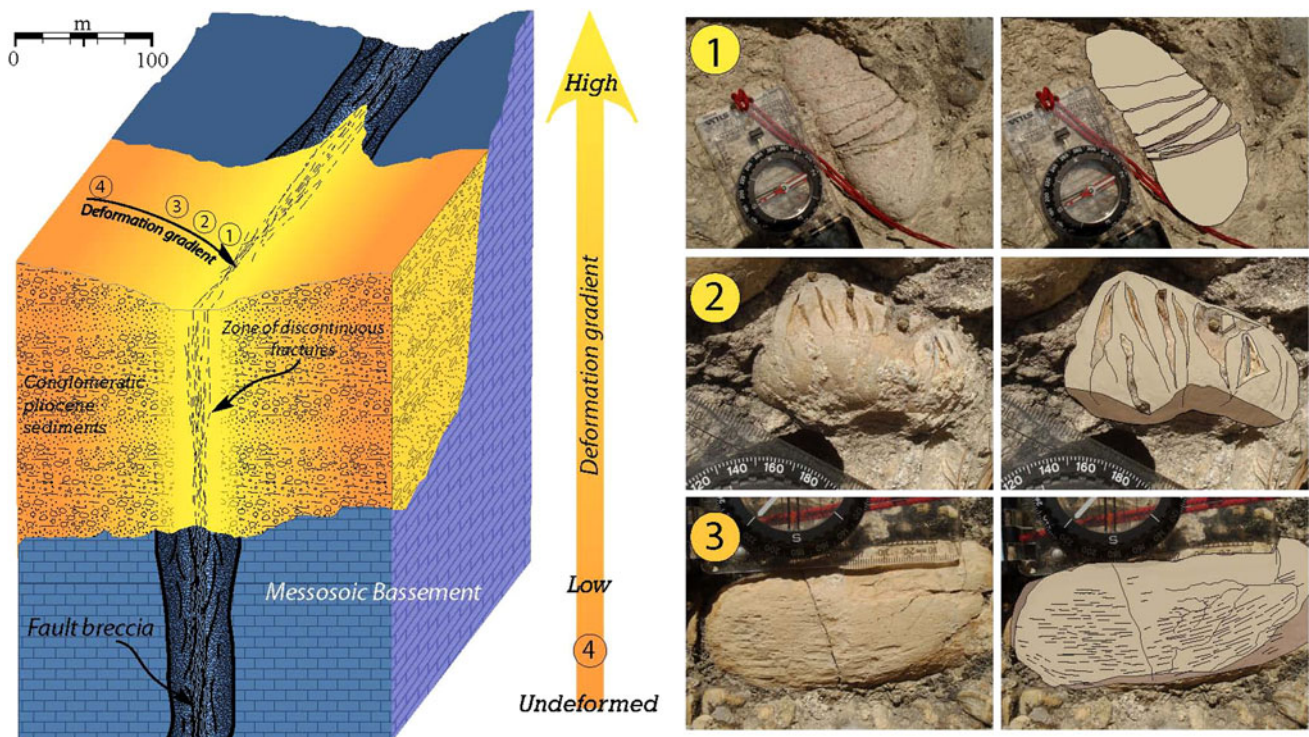


**Fig. 9** Block diagram schematically showing the distribution of deformation in conglomeratic sediments above a fault corridor cross-cutting the Mesozoic limestones. The deformation is characterized by a strain gradient, with a higher density of discontinuous fractures and strained pebbles in the centre (1), decreasing laterally by ~150 m to unstrained domains (4). In the central part, pebbles are fractured and offset (1), while the size of fractures decreases rapidly (non-offset pebbles are found at several tens of meters across (2), and at the

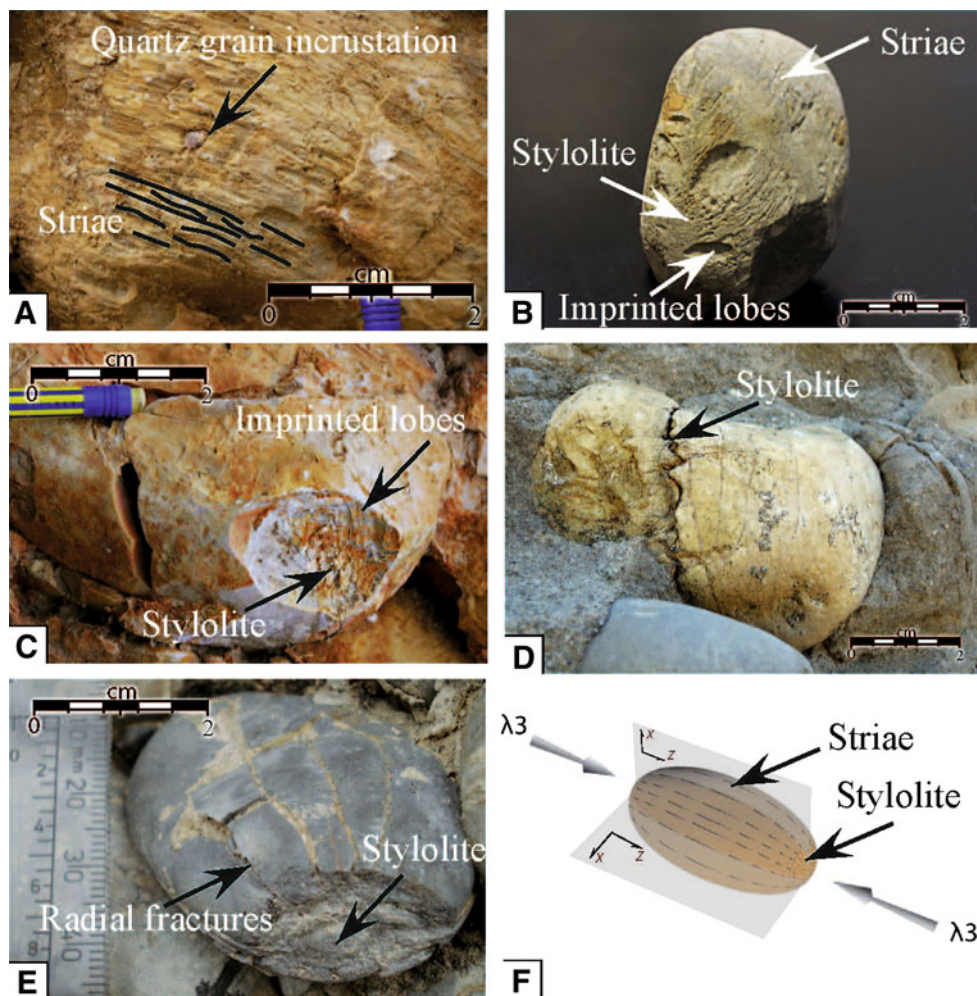
margin of the deformation zone, pebbles only show some joints and striae. Note that The fault corridor is larger and more accentuated in the Mesozoic basement, due to its initial pre-Pliocene age. Scattered and heterogeneous deformation that is expressed in the Pliocene molasse-type sediments above the fault suggests continuation of deformation after the Pliocene, but with less intensity and only minor offset

striated pebbles in a zone of about 300 m across above the fault zone affecting the Mesozoic basement (Fig. 9). All the observed examples of pebble deformation show pressure-dissolution features, summarized in Fig. 10 and Online Resource 2. These features include (1) striation on all sides of pebbles by incrustation of quartz sand grains, (2) stylolitic dissolution inside and at the surface of pebbles, (3) radial fracturing at the contact between pebbles. The analysis of the strained pebbles was conducted according to the method of Simon (2007). Striation orientations can be related to the intersection of the pebble surface with the so-called ‘motion plane’ defined by the compression and extension axes, Z and X (e.g., Campredon et al. 1977; Simon 2007). The computation of striation orientations is shown as rose diagrams on Figs. 10 and 11. The computation of all the measured pebbles across the area in one rose diagram shows a bimodal distribution of shortening directions centred on N156°E and N11°E (Fig. 11). The two directions coincide with the two previously defined fault directions defined in Sect. 3.4, corresponding to the trends of (1) the Donaréo Fault

corridor and (2) the direction of the St Blaise-Aspremont and Mont Chauve faults.

The plots of striation directions in the study area, locality by locality (Fig. 12), show that the direction of shortening of strained pebbles is globally controlled by these two fault directions. The pebbles are striated in the N160°E direction, parallel to the Donaréo Fault (rose diagrams 4, 5 and 10–14 in Fig. 12) or to the Nice Arc boundary (rose diagrams 1, 2 and 6–9 in Fig. 12). The two directions appear together at the junction between Donaréo Fault and boundary of the Nice Arc (rose diagrams 2, 3 and 10 in Fig. 12). Thus, it appears that the striation directions parallelize the faults. This bimodal distribution is compatible with the N–S shortening (N175°E), which is the bisector direction of conjugate N10°E sinistral and N155°E dextral faults. Apart from these two main directions, a minor proportion of striations with orientations between N10°E and N70°E is observed, and no striations perpendicular to the N–S direction have been measured. The dispersion in these values is ascribed to the irregularity of pebble surfaces on which the striations were measured,

**Fig. 10** Deformation features of strained Pliocene pebbles giving evidence of pressure-dissolution processes. **a** *Striated* pebbles showing incrustation of quartz sand grains. **b** Pebble *striated* on all sides. **c** Imprinted lobes on pebble surface corresponding to the trace of former neighbouring pebbles. **d** Stylolitic surface inside a pebble. **e** Radial fractures produced at the contact with a neighbouring pebble. **f** Schematic interpretative sketch explaining the deformation context. See also Online Resource 2 for detailed pressure-dissolution features observed on all sides of pebbles



and possible rotation of pebbles due to elongation parallel to the main fault directions. The absence of striations on EW-striking faces of pebbles is ascribed to the absence of grain matrix sliding, and pure dissolution during their stylolitic incrustation, in the direction perpendicular to  $\sigma_1$ . In contrast, on oblique faces, the formation of the striations is explained by friction of sand grains during their incrustation on pebble surface. We thus consider that striations related to pressure-dissolution processes are compatible with long-term stress loading in the Pliocene basin domain directly above the Mesozoic basement fault corridor, and do not reflect instantaneous sliding as striated faults.

#### 4 Discussion

The analysis of long-term deformation of potentially active fault systems is generally based on (1) geophysical analysis, mainly by seismology, to track its ongoing activity, and (2) the morphological and tectonic analysis of faults by geological investigation, to reconstruct its recent and long-

term history (e.g., Hippolyte and Dumont 2000; Cushing et al. 2008; Sani et al. 2009), and geochronology (e.g., Ritz et al. 2006). The problem posed by slow orogenic domains lies in the paucity of seismological information for the former and in the erosion of morphological displacements for the latter approach. Further, seismicity in these slow tectonics environments may be strongly influenced by external factors such as seasonal water charge and discharge in aquifers (Saar and Manga 2003). Thus, it might be difficult to interpret seismicity only in terms of active tectonics. In order to provide estimate for rates of displacements in the slow orogens, it is however important to constrain the long-term geological evolution of fault zones, which bear a seismic potential (e.g., Hippolyte 2001; Bonini et al. 2011). Such geological analysis would serve as a basis to identify risk areas in highly vulnerable zones, and for further focused seismic hazard investigations with combined high-resolution geophysical tools.

From the present case, on the south-western margin of the Alps, it appears that long-term displacement and tectonic behaviour of such active faults can be constrained by

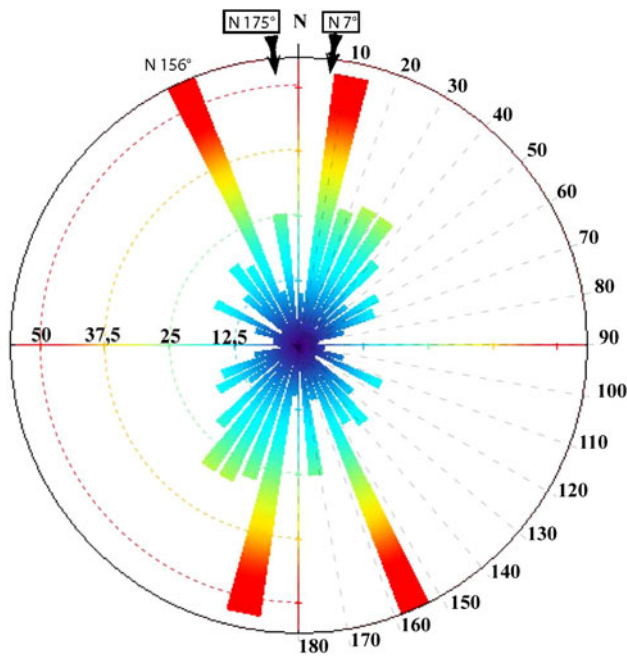


**Fig. 11** Rose diagram showing the azimuths of striations measured on >400 *strained* pebbles in the whole area. The computation of all the measured pebbles shows a bimodal distribution of shortening direction (N156°E and N11°E). The mean striation value of the whole measured dataset is N7°E, and the bisector direction of the two principal modes is of N175°E. The bimodal distribution is correlated with the two main fault directions (see Fig. 12). This data strongly suggests that pebble deformation is controlled by localization along the fault direction. Striations appear by pressure-dissolution processes due to the incrustation of quartz sand onto the pebble surface. The absence of any striations in the direction perpendicular to the main shortening axis reflects a pure stylolitic incrustation in the N–S direction, while oblique pebble surfaces undergo sliding + incrustation producing the striations

an approach combining (1) study of recent geological strata which may conserve traces of the deformation, (2) the use of DEM to outline the fault lineaments, which might be emphasized by erosion, and (3) the analysis of faults and strained pebbles to calculate paleostress directions.

#### 4.1 Deformation context of the Var Pliocene Basin (Nice area)

The combination of approaches used in this study show:

(1) DEM data bear a strong morphological imprint along a N20°E direction, the Donaréo stream. This direction also controls the turn of the Var valley, which is also deflected along the strike of the fault corridor (Fig. 3). The slope and water drainage anomalies evidence distinct erosional dynamics from the rest of the basin. These data highlight the role of the Donaréo Fault in the morphological shaping of the Var valley, despite the slow tectonics and relatively high erosion rate in these soft sediments.

- (2) Along the line of the Donaréo Fault, striated surfaces are preserved, which can be interpreted in terms of a N–S shortening direction. This shortening direction is in agreement with the focal mechanisms derived from seismologic data on the main events that occurred in the area (Courboulex et al. 2007; Béthoux et al. 2007; Jenatton et al. 2007).
- (3) The analysis of pebble deformation yields complementary information on deformation inside the main fault zones, and provides further insights into the kinematics of the faults. Two fault directions are shown to control the deformation of pebbles: the N20°E-trending, left-lateral, Donaréo Fault, and the N150°E-trending, right-lateral, Nice Arc boundary. Striated pebbles are mainly observed in the Pliocene basin domain directly above the fault corridor cross-cutting the Mesozoic basement. Striated pebbles witness pressure-dissolution processes coherent with long-term stress loading, and not instantaneous slip on fault surfaces.
- (4) The geometrical relationships between the faults and the basins, as emphasized in Sect. 3.2 show the presence of a positive flower structure, which argues for a transpressional strike-slip boundary along the western Nice Arc. This fault accommodates N–S compression and top-to-S displacement of cover units during the Miocene period (e.g., Schreiber et al. 2010; Sanchez et al. 2011a; Giannerini et al. 2011). The localization of the fault along the Var valley and the overall geometry are in good agreement with the idea of a thick-skin reactivation of a N–S fault in the crystalline basement. Regional-scale anisotropy is defined by N–S crustal faults in the Provence crystalline basement (e.g., Crevola 1997), related to transpressive deformation during the Variscan orogeny (Rolland et al. 2009; Corsini and Rolland 2009). These faults were firstly reactivated with extensional motion during the Oligocene phase of basin formation and volcanic activity (Biot volcanics), and were further reactivated by Recent and ongoing thick-skinned tectonics. Thick-skinned tectonics, and the absence of present-day cover-basement decoupling, is supported by: (1) the focal depth of earthquakes at ca. 5 km, i.e. well below the level of the basement-cover contact (2 km); (2) sealing of nappe contacts by Pliocene molasse-type sediments; (3) lack of decoupling indicated by similar apatite fission-track ages in crystalline basement and cover along the Argentera-Mercantour range since 8 Ma (Sanchez et al. 2011a).
- (5) Geometrical analysis of the relationships between faults and basins highlight some post-Pliocene reactivation, with vertical offset of about 100 m along the transpressional faults and displacement of 500 m of the depocenters of the basins (Figs. 4 and 13).

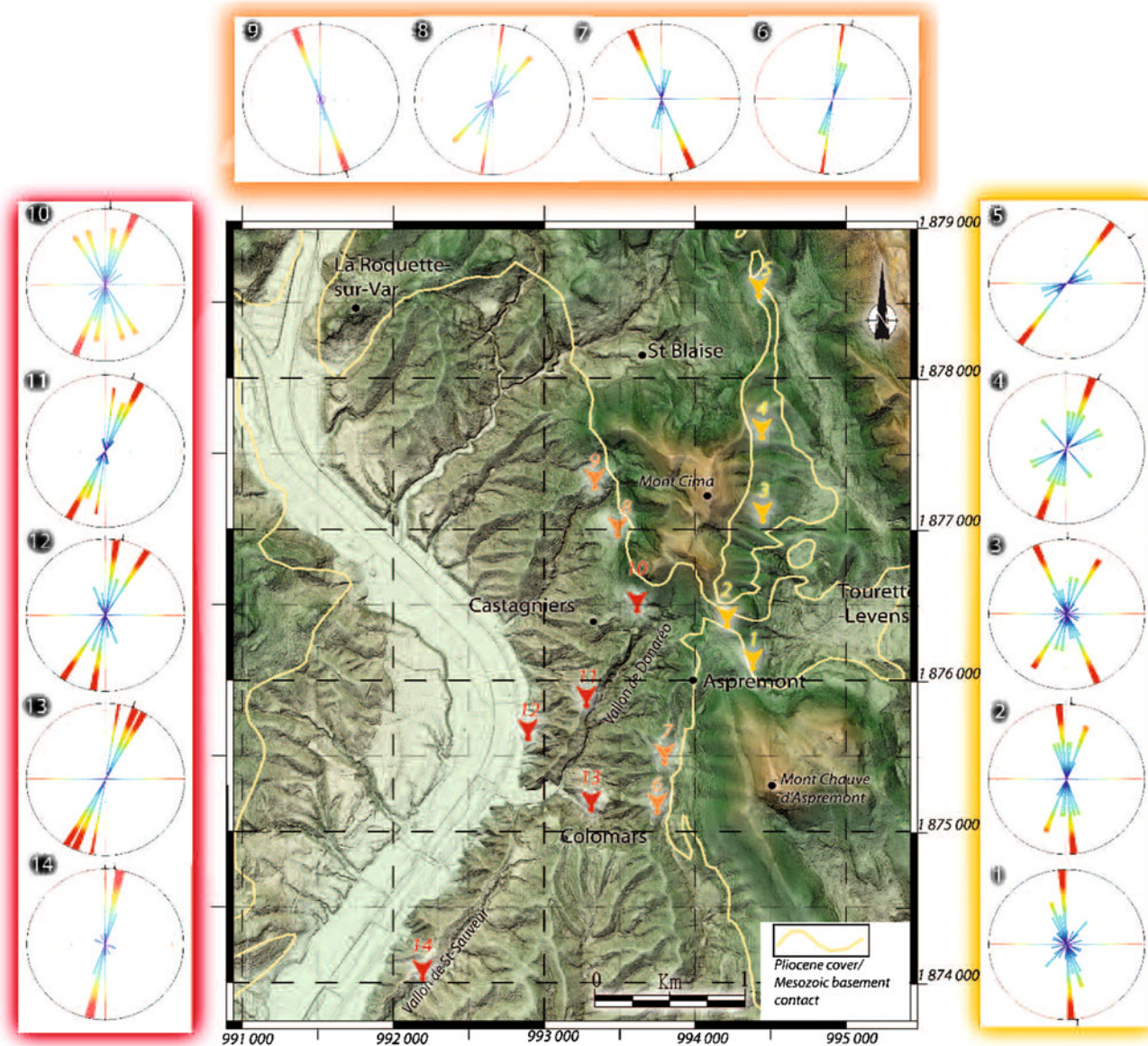


**Fig. 12** Rose diagrams of striation directions of measured strained pebbles, shown by locality. Note that the striation directions are mainly controlled by the main fault direction (N20°E–N30°E along

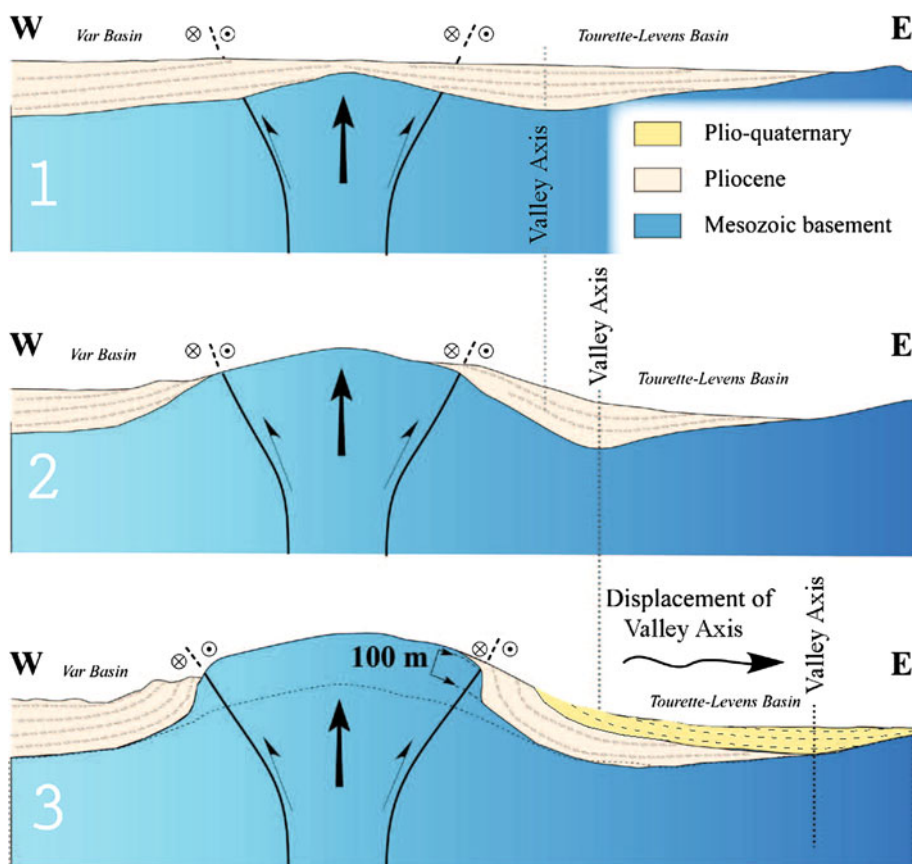
the Donaréo Fault and N150°E–N0° along the St Blaise Aspremont Fault), which is globally compatible with N–S shortening

These motions are in agreement with a continuous tectonic activity from the Miocene to the Pliocene and present. The total amount of displacement for 5 Ma (Pliocene to Present) is thus significantly lower than for the Jausiers-Tinée and Bercesio Faults in the Mercantour Range, which show local Quaternary displacements of up to ~30 m (Sanchez et al. 2010b, 2011a). Inferred potential geological hazard from offset-magnitude relationships is thus significantly less in the ‘peripheral’ Donaréo and St Blaise-Aspremont Faults, neighbouring Nice city, than in the ‘main’ Jausiers-Tinée Fault, bordering the Argentera-Mercantour range.

#### 4.2 Interpretation in terms of active tectonics

In terms of seismic hazard potential it is likely that the Donaréo Fault, and other faults with similar orientation such as the Peille-Laghet Fault, might still be currently active. This is suggested by the low-magnitude earthquake swarms along the Peille-Laghet Fault (Courboux et al. 2007). The focal mechanisms obtained by seismological analysis provide similar stress tensors to those obtained by the fault-striation inversion methods undertaken from the present field measurements. Observations in the Donaréo Fault suggest that it was active since at least 5 Ma and had a strong impact on the deformation of Pliocene to

**Fig. 13** Sketch evolutionary model for the activity of the St Blaise-Aspremont and Donaréo fault systems. (1) The Pliocene molasse-type sediments were deposited in submarine conditions after the Messinian crisis at ca. 5.3 Ma. The molasse-infilled incised valleys were formed during the Messinian crisis, and thus sealed the pre-Pliocene deformation. (2) Reactivation of the strike-slip system in Pliocene to Quaternary times resulted in basin axial valley migration to the side of the developing morphology. (3) A significant part of the uplift (a minimum of 100 m) is ascribed to tectonic movements along the faults, which resulted in the Pliocene verticalization



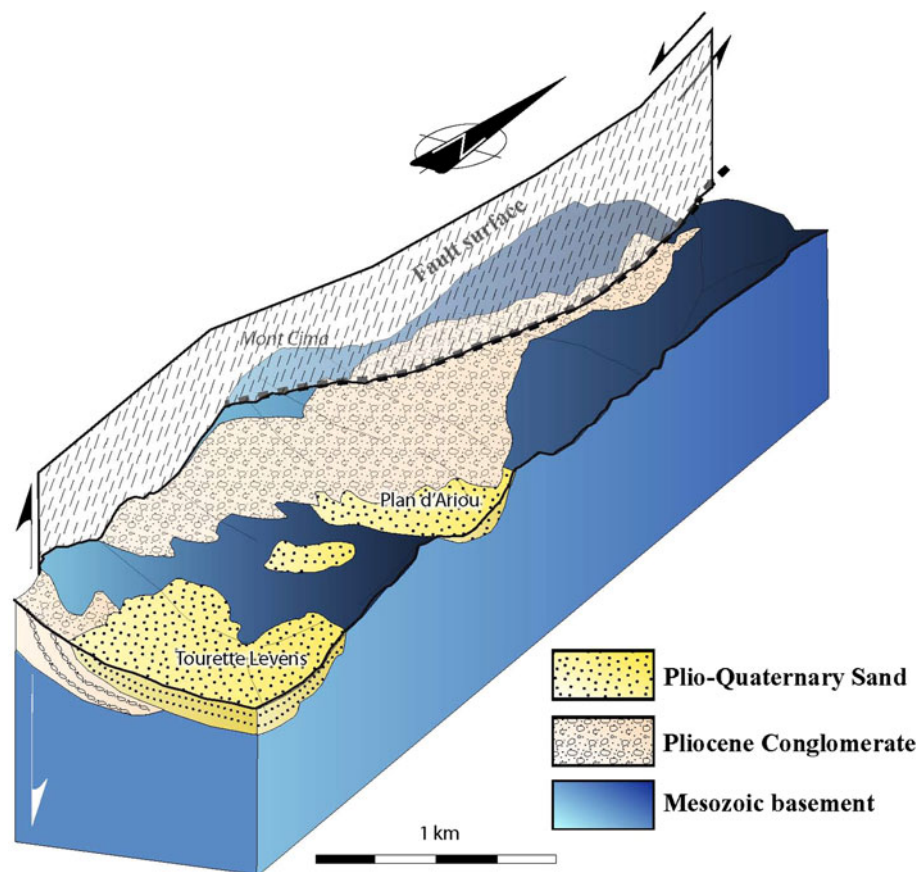
Quaternary sediments, and on the geomorphology of the present Var valley. Hence, continued activity up to the present time is probable. However, up to now, no seismicity has been evidenced for the Donaréo Fault, which could be explained by its very slow and aseismic character (see Sect. 4.3 below). At a regional scale, the Donaréo and Peille-Laghet Faults merge into a major active fault system along the Argentera-Mercantour range from Jausiers to Taggia (Fig. 2). The N140°E south-western boundary of the Argentera-Mercantour massif appears to have been active in the Quaternary and Holocene (Sanchez et al. 2010a; Darnault et al. 2012), with decametric right-lateral offset of morphologies, and is evidenced to be currently active in the seismological record (Jenatton et al. 2007). Our interpretation is thus that the left-lateral Donaréo and Peille-Laghet Faults must also be considered to be active, although peripheral to this main dextral Jausiers-Tinée-Taggia Fault system.

#### 4.3 Seismic versus aseismic behaviour of the active fault

The above observations suggest the active nature of the Donaréo Fault and the western boundary of the Nice Arc (St Blaise-Aspremont Fault), although the seismic versus aseismic character of some of the observed deformation

features is a matter of debate. The progressive strain gradient that is observed from the core to the rim of the Donaréo Fault corridor and along the western Nice Arc, and the absence of any continuous fault surface on scales above several meters in well exposed road sections (Fig. 9), argues for small displacements and for a deformation context dominated by pressure-dissolution processes. Such a context may be explained by (1) the permanence of maintained stress values during a long period of time without any seismic relaxation, (2) low-magnitude earthquakes or creep processes along the fault. Current seismological observations undertaken along various segments of the regional active fault network (Courboulex et al. 2007; Jenatton et al. 2007) may help resolve this issue. Along the Jausiers Fault, the slow tectonic motions are characterized by numerous (more than 14,000) low magnitude ( $M_w < 4$ ) earthquakes, defining a swarm along the fault strike (Jenatton et al. 2007). We propose that such low magnitude earthquake swarms may correspond to the nucleation of discontinuous fault planes such as those observed in the Donaréo Fault, as fault length-magnitude relationships predict ( $M_w < 4$ , Wells and Coppersmith 1994). Therefore, the numerous observed fault planes are indicative of a diffuse deformation in the superficial part of a more continuous fault cross-cutting the Mesozoic basement in the way drawn on the Fig. 9. The geometry of the fault below was mainly already acquired in the Miocene, and only

**Fig. 14** Block diagram derived from 3D-geological modelling using the BRGM software developed with the methods of Lajaunie et al. (1997). The 3D model illustrates the relationship of basin formation and strike-slip faulting along the western margin of the Nice Arc. Two superposed (Pliocene marine and Plio-Quaternary lacustrine) basins are emplaced along the fault runoff. Double unconformity is shown by relatively flat-lying Plio-Quaternary basin, tilted by about 40° above verticalized Pliocene molasse sealing the Messinian topography. These relationships are in agreement with basin migration during topographic building along the Mont Cima-Les Salettes mountains. In turn, topographic building is geometrically related to the location of the fault along the Mont Cima



partly reactivated after the Pliocene. The fact that pebbles underwent a deformation mainly by pressure-dissolution processes is in agreement with continuous deformation during prolonged periods of stress loading and rare seismogenic deformation (i.e., by rupture along faults). Ductile flow of sandy matrix and pebble reorganization accommodate most of strain. Such a style of deformation is in agreement with a low seismogenic potential.

#### 4.4 Geometry and slip rate of “slow-active” fault zones

The absence of any clear continuous fault surface running for more than 10 m in the Pliocene sediments argue for the absence of any major superficial earthquake event post-dating the Pliocene. However, Pliocene strata were tilted in places up to 90°. This observation argues for some significant differential vertical uplift of the Nice Arc (Mont Cima) with respect to the basin after the Pliocene. It is clear from the basal relationship of these later lacustrine sediments (Figs. 4b and 14) that they infilled a valley that migrated more to the east of the main Messinian valley centre by ca. 500 m. The eastward migration of the valley is ascribed to uplift and slope building along Mont Cima. Thus, it appears that active deformation has been prolonged through time and

explains the setting of the Plio-Quaternary intramontane basin. From the geometrical relationships on cross-sections drawn across the Nice Arc, a minimum 100 m displacement is invoked from the tilting of (post-Messinian) Pliocene beds and uplift of the Messinian basal unconformity. This motion is acquired after the formation of the basal unconformity, whose age is constrained at about 5.3 Ma (Clauzon et al. 1996 and references therein). These geometrical and temporal constraints provide a minimum vertical uplift rate of  $0.02 \text{ mm a}^{-1}$ . The overall structure drawn in geological cross-section, Fig. 4b, agrees with a positive flower-type structure formed in a strike-slip context. However, the combination of dextral and sinistral motions shown by the fracture analysis is also in favour of conjugate fault splays: namely, the N20°E sinistral Donaréo Fault and the N150°E dextral St Blaise-Aspremont Fault. Given an average striation pitch of 30°N on the main Donaréo Fault, horizontal slip rates of  $\sim 0.03 \text{ mm a}^{-1}$  are likely on the boundary of the Nice Arc from Pliocene to Present.

## 5 Conclusion

The peripheral fault network of the south-western Alps in the Nice area has been investigated by a multi-disciplinary

geological approach. This study shows that geomorphology preserves the trace of the recent fault displacements even if erosion acts faster than tectonic slip. Fault analysis indicates a constant stress regime over a long period of time (>5 Ma), fully compatible with the current stress state derived from focal mechanisms. This data provides an insight into the geological signature of low-magnitude ( $M_w < 4$ ) seismic swarms, which is probably characterized by discontinuous small-scale (m-10 m) faults in the field, focussed in a corridor less than 100 m across. The study of pebbles provides insights into the permanence of long-lasting phases of pressure-dissolution deformation and rare seismogenic deformation, which is interpreted as a potentially long time recurrence and moderate magnitude for related earthquakes. Consequently, on the basis of these geological observations, we propose that such "slow-active" faults bear a very low hazard potential, with a seismic behaviour mostly featured by episodic seismic swarms of low magnitude ( $M_w < 4$ ) earthquakes. Even so, it remains essential to investigate the influence of such low, but shallow, seismicity on seismic risk assessment in the neighbouring, and even locally overlying, urban area, if site effects and vulnerability are being considered. Furthermore, in terms of seismic hazard potential, it is likely that the apparently minor sinistral Donaréo and Peille-Laghet Faults merge into a major dextral active fault system along the Argentera-Mercantour range from Jausiers to Taggia, in the frontal part of the Alpine orogen.

**Acknowledgments** The authors wish to thank the University of Nice Sophia Antipolis for its support in providing the first author with a PhD fellowship. The CETE-Méditerranée group is thanked for its collaboration and support, and in this context we warmly thank A. M. Duval and E. Bertrand for many fruitful discussions. The Nice city CANCA is acknowledged for providing the high resolution DEM data. The authors warmly thank the help of Jenny Trevisan for her help in the computation of the DEM, and Marc Hässig for the checking of the English language. We are grateful to the reviewers N. Bellahsen and A. G. Milnes for their comments and suggestions, which led to a considerably improved manuscript.

## References

- Angelier, J. (1990). Inversion of field data in fault tectonics to obtain the regional stress—III. A new rapid direct inversion method by analytical means. *Geophysical Journal International*, *103*, 363–376.
- Arthaud, F. (1969). Méthode de détermination graphique des directions de raccourcissement, d'allongement et intermédiaire d'une population de failles. *Bulletin de la Société Géologique de France*, *11*, 729–737.
- Baietto, A., Perello, P., Cadoppi, P., & Martinotti, G. (2009). Alpine tectonic evolution and thermal water circulations of the Argentera Massif (South-Western Alps). *Swiss Journal of Geosciences*, *102*, 223–245. doi:10.1007/s00015-009-1313-5.
- Baue, V., Rolland, Y., Sanchez, G., Giannerini, G., Schreiber, D., Corsini, M., Perez, J.-L., Romagny, A. (2011). Characterization of active fault systems in slow orogenic domains, example of the Alpine Front in SE France and insights for geological hazard, *10th Alpine workshop "CorseAlp2011"*, p.11. [http://www.corsealp2011.it/doc/corse\\_alp\\_absrats.pdf](http://www.corsealp2011.it/doc/corse_alp_absrats.pdf).
- Béthoux, N., Sue, C., Paul, A., Virieux, J., Fréchet, J., Thouvenot, F., & Cattaneo, M. (2007). Local tomography and focal mechanisms in the south-western Alps: Comparison of methods and tectonic implications. *Tectonophysics*, *432*(1–4), 1–19.
- Bigot-Cormier, F., Sage, F., Sosson, M., Deverchère, J., Ferrandini, M., Guennoc, P., et al. (2004). Pliocene deformation of the north-Ligurian margin (France): consequences of a south-Alpine crustal thrust. *Bulletin de la Société Géologique de France*, *175*, 197–211.
- Bonini, M., Sani, F., Moratti, G., & Benvenuti, M. G. (2011). Quaternary evolution of the Lucania Apennine thrust front area (Southern Italy), and its relations with the kinematics of the Adria Plate boundaries. *Journal of Geodynamics*, *51*, 125–140. doi:10.1016/j.jog.2010.01.010.
- Campredon, R., Franco, M., Giannerini, G., Gigot, P., Irr, F., Lanteaule, M., et al. (1977). Les déformations de conglomérats pliocènes de l'Arc de Nice – Chaînes subalpines méridionales. *Compte rendu sommaire, Bulletin de la Société Géologique de France*, *2*, 77–78.
- Cederbom, C. E., Sinclair, H. D., Schlunegger, F., & Rahn, M. K. (2004). Climate-induced rebound and exhumation of the European Alps. *Geology*, *32*, 709–712.
- Champagnac, J. D., Molnar, P., Anderson, R. S., Sue, C., & Delacou, B. (2007). Quaternary erosion-induced isostatic rebound in the western Alps. *Geology*, *35*, 195–198.
- Clauzon, G., Suc, J. P., Gautier, F., Berger, A., & Loutre, M. F. (1996). Alternate interpretation of the Messinian salinity crisis: controversy resolved? *Geology*, *24*, 363–366. doi:10.1130/0091-7613.
- Collombet, M., Thomas, J. C., Chauvin, A., Tricart, P., Bouillin, J. P., & Gratier, J. P. (2002). Counterclockwise rotation of the western Alps since the Oligocene: new insights from paleomagnetic data. *Tectonics*, *21*(4), 14.1–14.15.
- Corsini, M., & Rolland, Y. (2009). Late evolution of the southern European Variscan belt: exhumation of the lower crust in a context of oblique convergence. *Compte rendu Geoscience*, *341*, 214–223.
- Corsini, M., Ruffet, G., & Caby, R. (2004). Alpine and late hercynian geochronological constraints in the Argentera Massif (Western Alps). *Eclogae Geologicae Helvetiae*, *97*, 3–15.
- Courboulex, F., Larroque, C., Deschamps, A., Kohrs-Sansorny, C., Gélis, C., Got, J. L., et al. (2007). Seismic hazard on the French Riviera: observations, interpretations and simulations. *Geophysical Journal International*, *170*, 387–400.
- Crescentini, L., Amoroso, A., & Scarpa, R. (1999). Constraints on slow earthquake dynamics from a Swarm in Central Italy. *Science*, *10*, 2132–2134. doi:10.1126/science.286.5447.2132.
- Crevola, G. (1997). Sur l'origine des virgations des Maures occidentales (Var, France). *Bulletin de la Société Géologique de France*, *168*, 685–687.
- Cushing, E. M., Bellier, O., Nechtschein, S., Sébrier, M., Lomax, A., Volant, P., et al. (2008). A multidisciplinary study of a slow-slipping fault for seismic hazard assessment: the example of the Middle Durance Fault (SE France). *Geophysical Journal International*, *172*, 1163–1178.
- Darnault, R., Rolland, Y., Boulès, D., Braucher, R., Sanchez, G., Revel, M., et al. (2012). Timing of the last deglaciation revealed by receding glaciers at the Alpine-scale: impact on mountain geomorphology. *Quaternary Science Reviews*, *31*, 127–142. doi:10.1016/j.quascirev.2011.10.019.
- Delacou, B., Sue, C., Nocquet, J.-M., Champagnac, J.-D., Allanic, C., & Burkhard, M. (2008). Quantification of strain rate in the

- Western Alps using geodesy: comparisons with seismotectonics. *Swiss Journal of Geosciences*, *101*, 377–385.
- Foeken, J. P. T., Dunai, T. J., Bertotti, G., & Andriessen, P. A. M. (2003). Late Miocene to present exhumation in the Ligurian Alps (Southwest Alps) with evidence for accelerated denudation during the Messinian salinity crisis. *Geology*, *31*(9), 797–800.
- Galli, P., Giaccio, B., & Messina, P. (2010). The 2009 central Italy earthquake seen through 0.5 Myr-long tectonic history of the L'Aquila faults system. *Quaternary Science Reviews*, *29*, 3768–3789. doi:10.1016/j.quascirev.2010.08.018.
- Giannerini, G., Sanchez, G., Schreiber, D., Lardeaux, J.-M., Rolland, Y., Bellando de Castro, A., et al. (2011). Geometry and sedimentary evolution of the transpressive Roquebrune-Cap Martin basin: implications on kinematics and timing of the Nice arc deformation during Miocene times, SW Alps. *Bulletin de la Société Géologique de France*, *182*, 493–506.
- Hippolyte, J. C. (2001). Palaeostress and neotectonic analysis of sheared conglomerates: southwest Alps and Southern Apennines. *Journal of Structural Geology*, *23*, 421–429.
- Hippolyte, J.-C., & Dumont, T. (2000). Identification of Quaternary thrusts, folds and faults in a low seismicity area: examples in the Southern Alps (France). *Terra Nova*, *12*, 156–162.
- Hu, C.-J., & Angelier, J. (2004). Stress permutations: Three-dimensional distinct element analysis accounts for a common phenomenon in brittle tectonics. *Journal of Geophysical Research*, *109*, B09403. <http://dx.doi.org/10.1029/2003JB002616>.
- Irr, E. (1984). *Paléoenvironnements et évolution géodynamique néogènes et quaternaires de la bordure nord du bassin méditerranéen occidental, un système de pente de la paléomarge Liguro-Provençale*. Thèse de Doctorat d'Etat: Université de Nice. 464p.
- Ivaldi, J. P., & Guardia, P. (1986). Early Paleogene deformation in South-eastern slipped sedimentary cover of the Argentera Massif (French Maritime Alps). *Comptes Rendus de l'Académie des sciences Série II*, *303*, 1605–1610.
- Jenatton, L., Guiguet, R., Thouvenot, F., & Daix, N. (2007). The 16,000 event 2003–2004 earthquake swarm in Ubaye (French Alps). *Journal of Geophysical Research*, *112*, B11304. doi:10.1029/2006JB004878.
- Kirby, E., & Whipple, K. (2001). Quantifying differential rock-uplift rates via stream profile analysis. *Geology*, *29*, 415–418. doi:10.1130/0091-7613.
- Lajaunie, C., Courrioux, G., & Manuel, L. (1997). Foliation fields and 3D cartography in geology: principles of a method based on potential interpolation. *Mathematical Geology*, *29*, 571–584. doi:10.1007/BF02775087.
- Lardeaux, J. M., Schwartz, S., Tricart, P., Paul, A., Guillot, S., Béthoux, N., et al. (2006). A crustal-scale cross-section of the south-western Alps combining geophysical and geological imagery. *Terra Nova*, *18*, 412–422. doi:10.1111/j.1365-3121.2006.00706.x.
- Larroque, C., Delouis, B., Godel, B., & Nocquet, J.-M. (2009). Active deformation at the southwestern Alps-Ligurian basin junction (France-Italy boundary): evidence for recent change from compression to extension in the Argentera massif. *Tectonophysics*, *467*, 22–34. doi:10.1016/j.tecto.2008.12.013.
- Larroque, C., Delouis, B., Hippolyte, J. C., Deschamps, A., Lebourg, T., Courboulex, F., et al. (2011). Joint multidisciplinary study of the Saint-Sauveur-Donareo fault (lower Var valley, French Riviera): a contribution to seismic hazard assessment in the urban area of Nice. *Bulletin de la Société Géologique de France*, *182*, 323–336.
- Ritz, J.-F., Vassallo, R., Braucher, R., Brown, E., Carretier, S., & Bourlès, D. (2006). Using in situ-produced  $^{10}\text{Be}$  to quantify active tectonics in the Gurvan Bogd mountain range (Gobi-Altay, Mongolia). *Geol. Soc. Am Special Paper*, *415*, 87–110.
- Rolland, Y., Corsini, M., & Demoux, A. (2009). Metamorphic and structural evolution of the Maures-Tanneron massif: evidence of syntaxial Himalayan-type doming and mantle-crust magma mixing along the SE Variscan chain transpressive margin. *Bulletin de la Société géologique de France*, *180*, 217–230.
- Saar, M. O., & Manga, M. (2003). Seismicity induced by seasonal groundwater recharge at Mt. Hood, Oregon. *Earth and Planetary Science Letters*, *214*, 605–618.
- Sanchez, G., Rolland, Y., Corsini, M., Braucher, R., Bourlès, D., Arnold, M., et al. (2010a). Relationships between tectonics, slope instability and climate change: cosmic ray exposure dating of active faults, landslides and glacial surfaces in the SW Alps. *Geomorphology*, *117*, 1–13.
- Sanchez, G., Rolland, Y., Corsini, M., Jolivet, M., Bricaud, S., Carter, A. (2011a). Exhumation controlled by transcurrent tectonics: the Argentera-Mercantour massif (SW Alps). *Terra Nova*, in press.
- Sanchez, G., Rolland, Y., Corsini, M., Oliot, E., Goncalves, P., Schneider, J., et al. (2011b). Dating Low-Temperature deformation by  $^{40}\text{Ar}/^{39}\text{Ar}$  on white mica, insights from the Argentera-Mercantour Massif (SW Alps). *Lithos*,. doi:10.1016/j.lithos.2011.03.009.
- Sanchez, G., Rolland, Y., Schreiber, D., Giannerini, G., Corsini, M., & Lardeaux, J.-M. (2010b). The active fault system of SW Alps. *Journal of Geodynamics*, *49*, 296–302.
- Sani, F., Bonini, M., Piccardi, L., Vannucci, G., Delle Donne, D., Benvenuti, M., et al. (2009). Late Pliocene-Quaternary evolution of outermost hinterland basins of the Northern Apennines (Italy), and their relevance to active tectonics. *Tectonophysics*, *476*, 336–356. doi:10.1016/j.tecto.2008.12.012.
- Schreiber, D., Lardeaux, J.-M., Martelet, G., Courrioux, G., & Guillen, A. (2010). 3-D modelling of Alpine Mohos in Southwestern Alps. *Geophysical Journal International*, *180*(3), 961–975.
- Segall, P., & Pollard, D. D. (1980). Mechanics of Discontinuous Faults. *Journal of Geophysical Research*, *85*, 4337–4350. doi:10.1029/JB085iB08p04337.
- Simon, J. L. (2007). Analysis of solution lineations in pebbles: kinematical vs. dynamical approaches. *Tectonophysics*, *445*, 337–352. doi:10.1016/j.tecto.2007.09.003.
- Sue, C., & Tricart, P. (2003). Neogene to ongoing normal faulting in the inner western Alps: a major evolution of the late alpine tectonics. *Tectonics*, *22*, 1–25.
- Tapponnier, P. (1977). Evolution tectonique du système alpin en Méditerranée: poinçonnement et écrasement rigide-plastique. *Bulletin de la Société Géologique de France*, *7*, 437–460.
- Vialon, P., Rochette, P., & Ménard, G. (1989). Indentation and rotation in the Western Alpine arc. *Geological Society Special Publications*, *45*, 329–338.
- Wells, D. L., & Coppersmith, K. J. (1994). New empirical relationships among magnitude, rupture length, rupture width, rupture area, and surface displacement. *Bulletin of the Seismological Society of America*, *84*, 974–1002.